Angewandte Chemie
Eine Zeitschrift der Gesellschaft Deutscher Chemiker

Supporting Information

A Mechanically Actuating Carbon-Nanotube Fiber in Response to Water and Moisture

*Sisi He, Peining Chen, Longbin Qiu, Bingjie Wang, Xuemei Sun, Yifan Xu, and Huisheng Peng**

anie_201507108_sm_miscellaneous_information.pdf
anie_201507108_sm_Movie_S1.avi
anie_201507108_sm_Movie_S2.avi
anie_201507108_sm_Movie_S3.avi
anie_201507108_sm_Movie_S4.avi

This PDF file includes:

Captions for Movies S1 to S4
Figures S1 to S19
Tables S1 to S2

Fabrication of the smart window and louver.

The windows were made of papers with the length of 6 cm and the width of 4 cm. Take the left window for example. A 10 cm-long HSF twisted from ten HPFs was first fixed on the right side of the window using the adhesive tape. The upper section was used to come into contact with water. Two ends of the fiber were then fixed on the frame to fabricate a smart window (Figure S19).

The louver was made of five papers. The length and the width of each paper were 6.8 cm and 1 cm, respectively. Take one unit of the louver for example. A 10 cm-long HSF twisted from ten HPFs was first fixed on the middle of each paper using the adhesive tape. Two ends of the fiber were then fixed on a frame (Figure S20).

Captions for supporting videos

Movie S1. Clockwise and anti-clockwise rotations of an HSF twisted from ten-ply HPFs upon contacting with a water droplet (length of ~7 mm). The metal paddle was 23,200 times heavier than the fiber.

Movie S2. A smart window in response to water. An HSF that twisted from ten-ply HPFs was fixed at the backside of a window where the upper section was exposed to generate rotations. The window was opened when the upper section of the fiber contacted a water droplet, while it was closed after removal of the water droplet.

Movie S3. A smart louver in response to moisture. An HSF that twisted from ten-ply HPFs was fixed at the backside of a louver where the left section was exposed to generate rotations. The louver was gradually opened with the increasing humidity from 25% to 80% at room.

Movie S4. A smart window in response to the change of weather. An HSF that twisted from ten-ply HPFs was fixed at the front of a window where the lower section was exposed to generate rotations. The window was opened in a sunny day and automatically closed due to the rotary actuation generated by the fiber upon raining, while it was opened again when raining stopped.

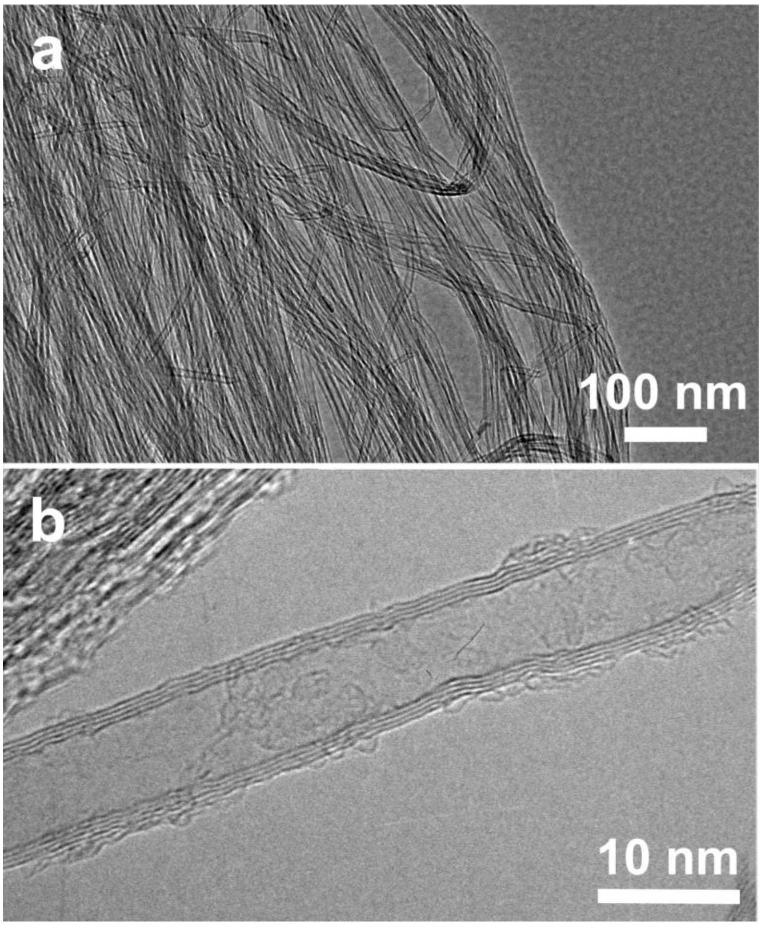

Figure S1. TEM images of CNTs at low (**a**) and high (**b**) magnifications prior to an oxygen plasma treatment.

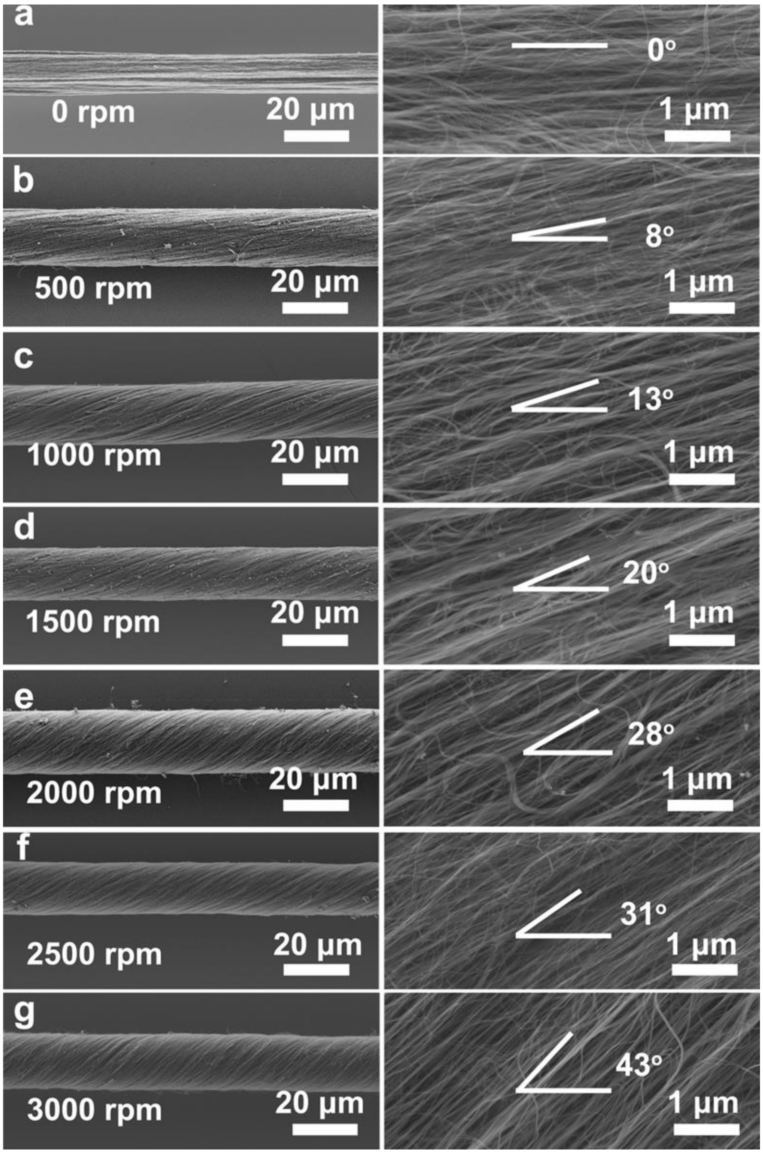

Figure S2. SEM images of CNT fibers with increasing helical angles.

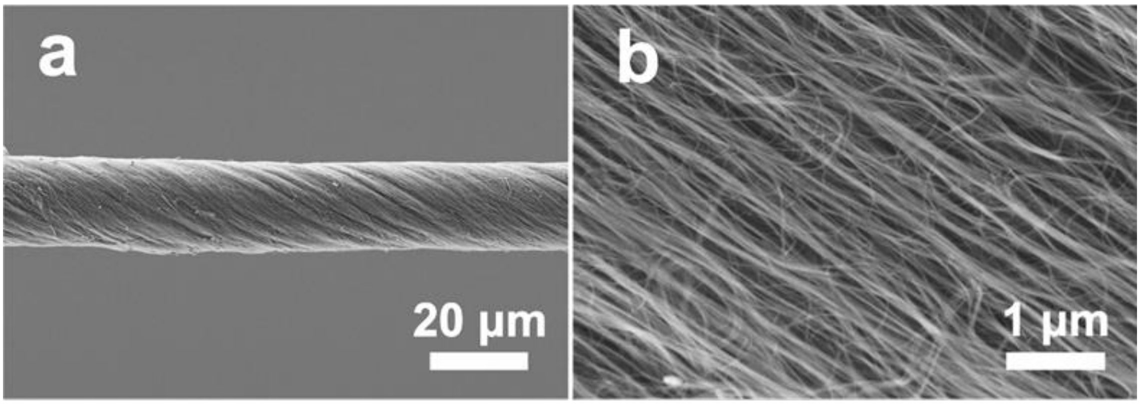

Figure S3. SEM images of a right-handed CNT fiber at low (**a**) and high (**b**) magnifications.

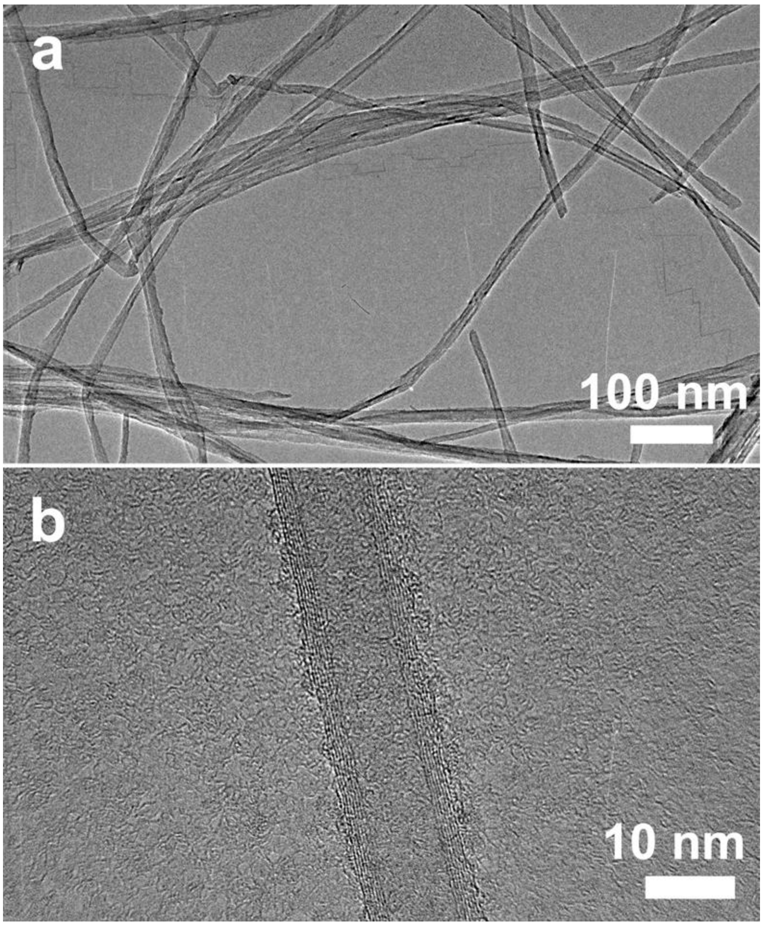

Figure S4. TEM images of CNTs at low (**a**) and high (**b**) magnifications after an oxygen plasma treatment.

Figure S5. Photograph of a roll of a continuous HPF after an oxygen plasma treatment.

Table S1. Carbon and oxygen contents of CNT fibers after plasma treatments with different powers and times.

Power	0 W	100 W	200 W	300 W	400 W	300 W	300 W
Time	0 min	15 min	15 min	15 min	15 min	30 min	45 min
C/wt%	96.8	94.4	93.7	89.1	88.2	87.8	82.5
O/wt%	3.2	5.6	6.3	10.9	11.8	12.2	17.5

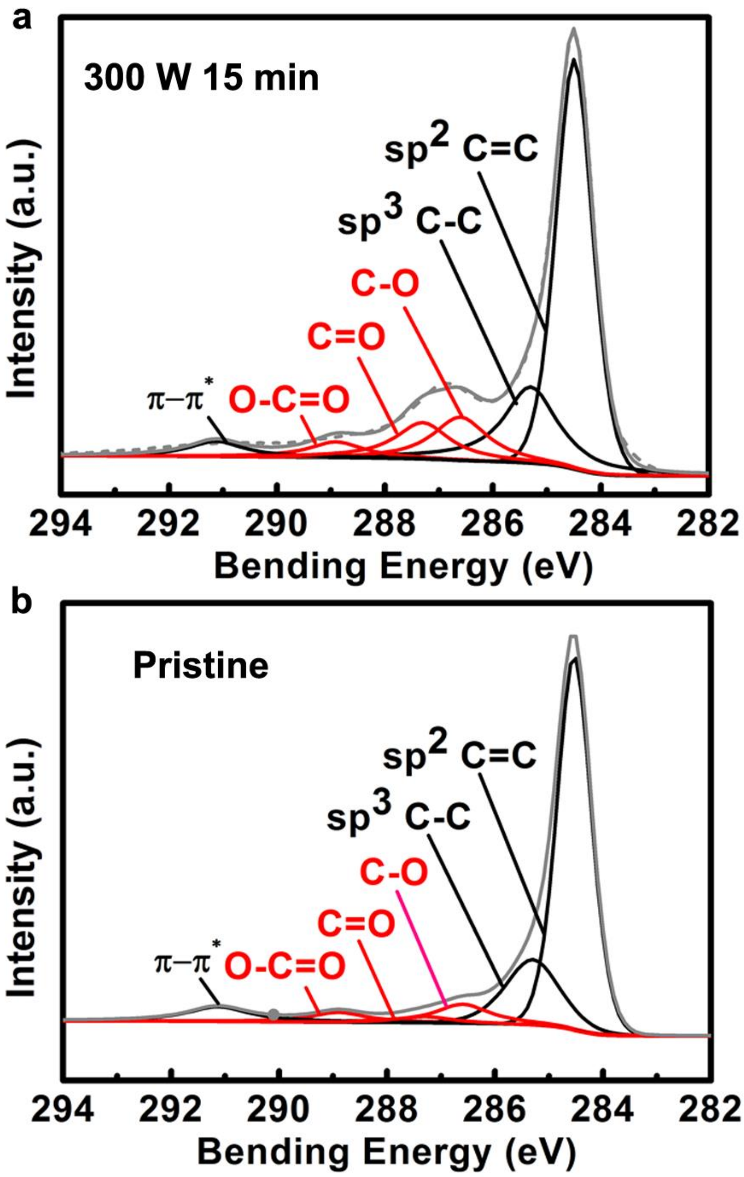

Figure S6. Deconvolution of the X-ray photoelectron spectroscopy C 1s peaks and the assigned bonds of an HPF at an oxygen content of 10.9 wt% (**a**) and pristine fiber (**b**).

Table S2. Relative sub-peak area of C 1s of the pristine fiber and modified fibers with increasing oxygen contents.

Oxygen content (wt%)	sp^2 C=C	sp^3 C-C	C-O	C=O	O-C=O	π-π*
3.2	63.0	17.8	7.1	1.8	3.7	6.7
10.9	52.6	20.1	9.9	9.2	4.2	4.1
17.6	48.5	20.6	10.2	12.0	4.8	3.9

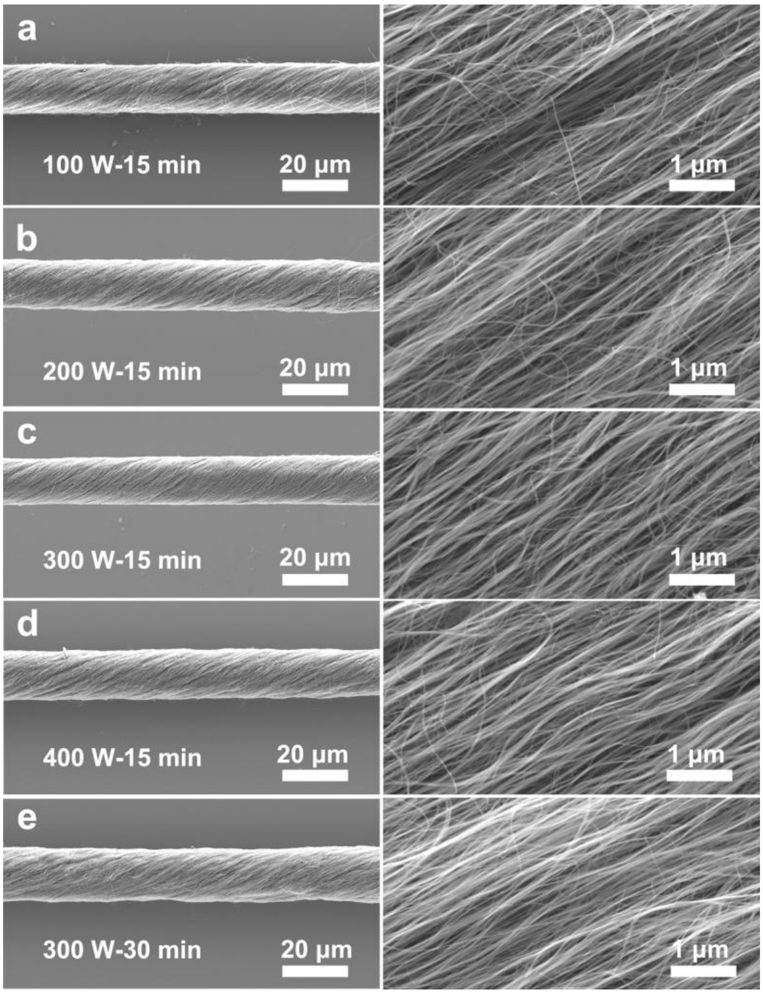

Figure S7. SEM images of HPFs at low and high magnifications with increasing oxygen contents of 5.6 wt% (**a**), 6.3 wt% (**b**), 10.9 wt% (**c**), 11.8 wt% (**d**) and 12.2 wt% (**e**).

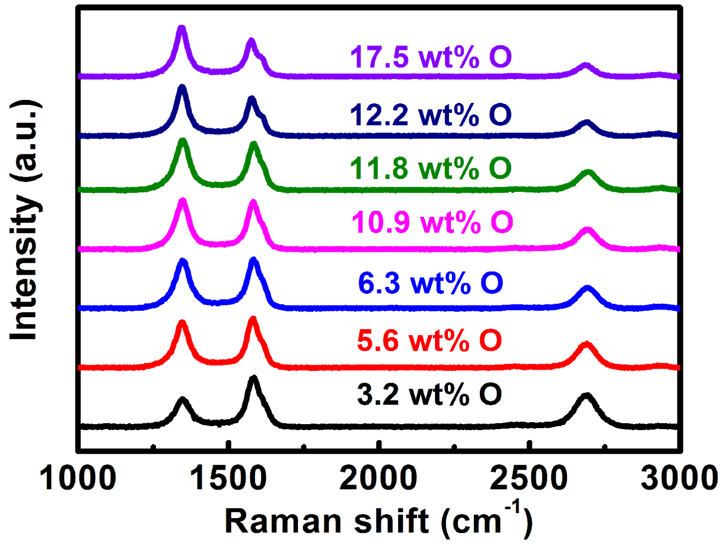

Figure S8. Raman spectra of HPFs with increasing oxygen contents.

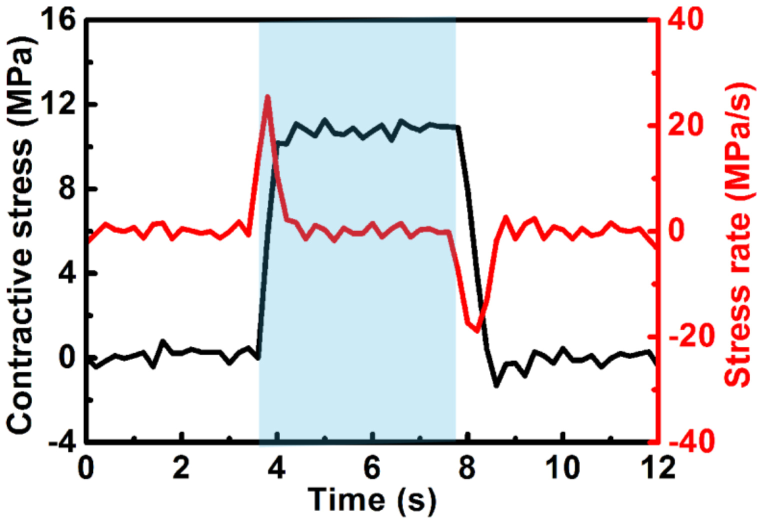

Figure S9. A typical contractive stress curve (black line) and the corresponding stress rate curve (red line) of an HPF upon absorption and removal of a water droplet.

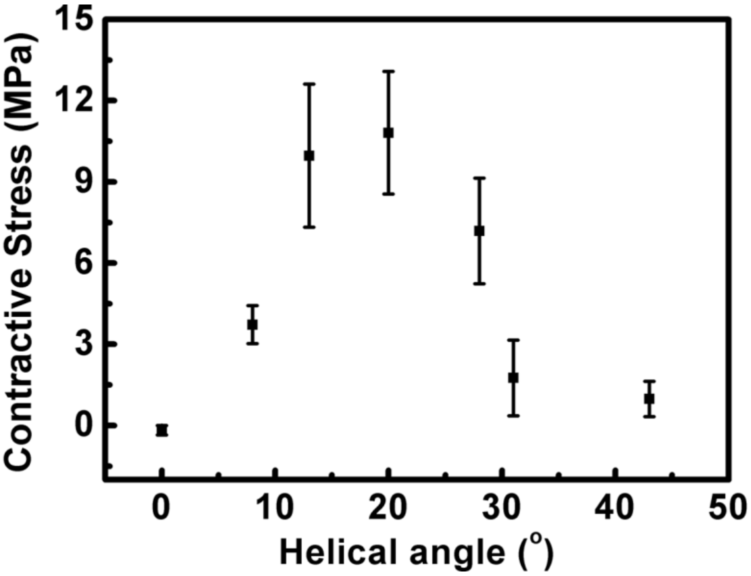

Figure S10. Dependence of contractive stress on helical angle. The fibers shared an oxygen content of 10.9 wt%.

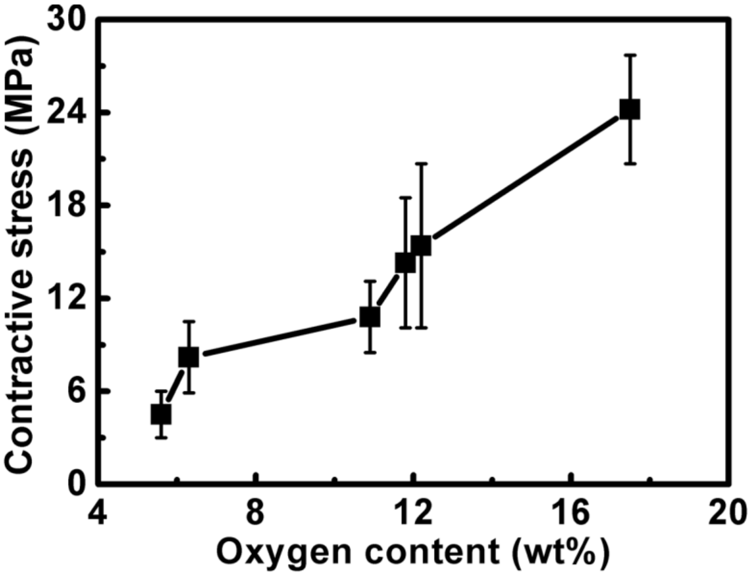

Figure S11. Dependence of contractive stress on oxygen content.

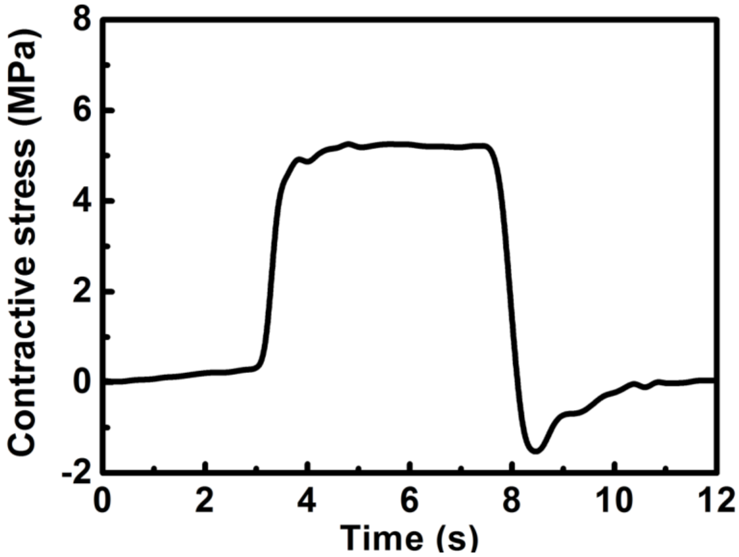

Figure S12. Response to ethanol for the bare CNT fiber.

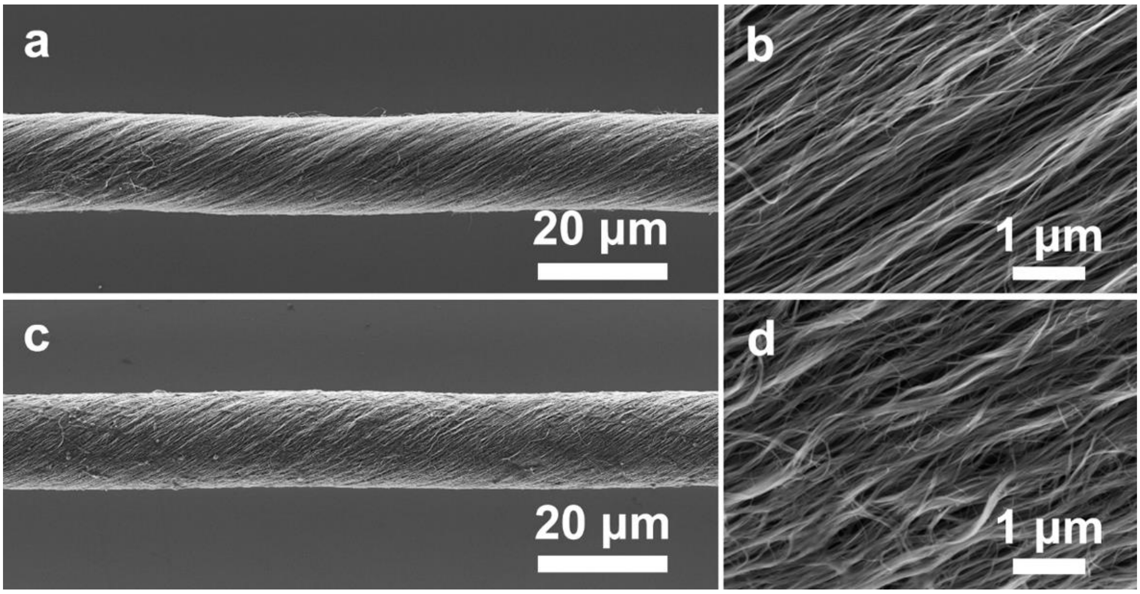

Figure S13. SEM images of the HPF before (**a**, **b**) and after (**c**, **d**) soaking in water for 240 h.

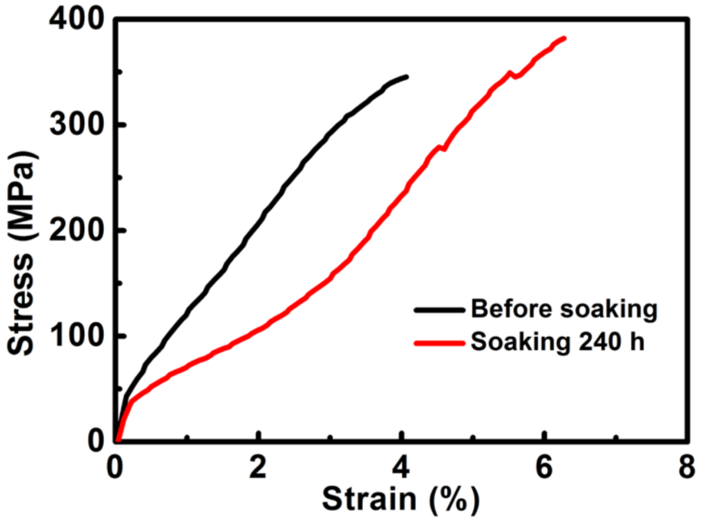

Figure S14. Stress-strain curves of the HPF before and after soaking in water for 240 h.

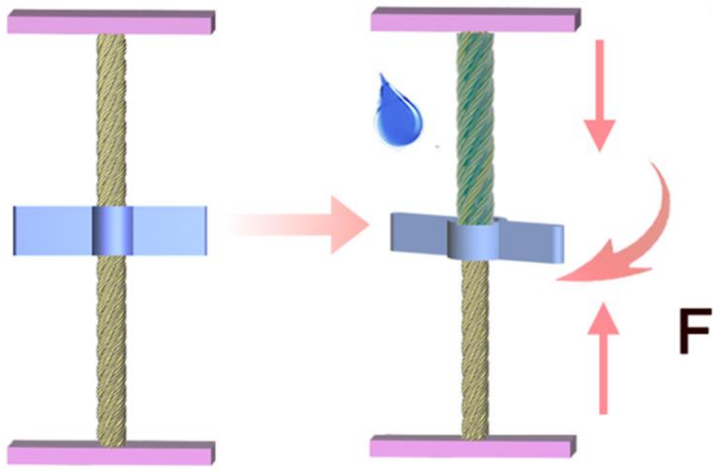

Figure S15. Schematic illustration to the experimental setup for the contractive actuation and rotatory actuation, respectively. The paddle was fixed at the middle of a two-end-tethered fiber.

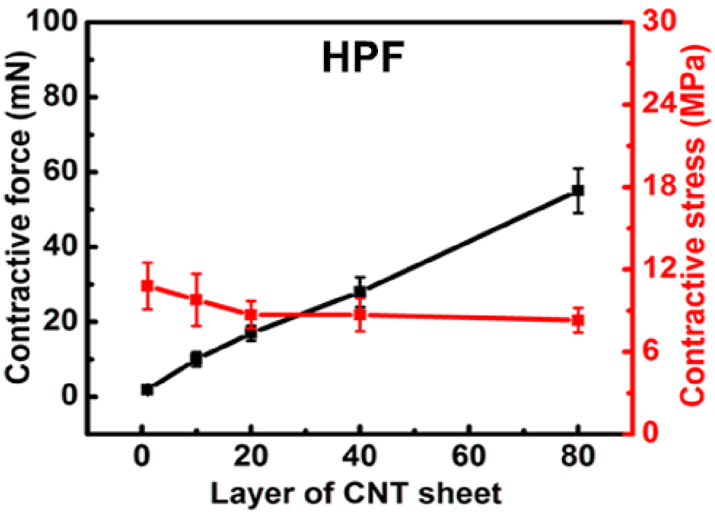

Figure S16. Dependence of contractive force (black line) and stress (red line) generated by the HPF on the layer number of stacked CNT sheet.

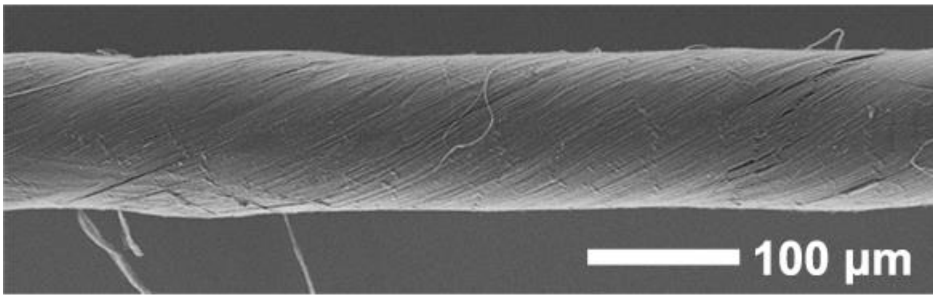

Figure S17. An HPF twisted from eighty layers of CNT sheet.

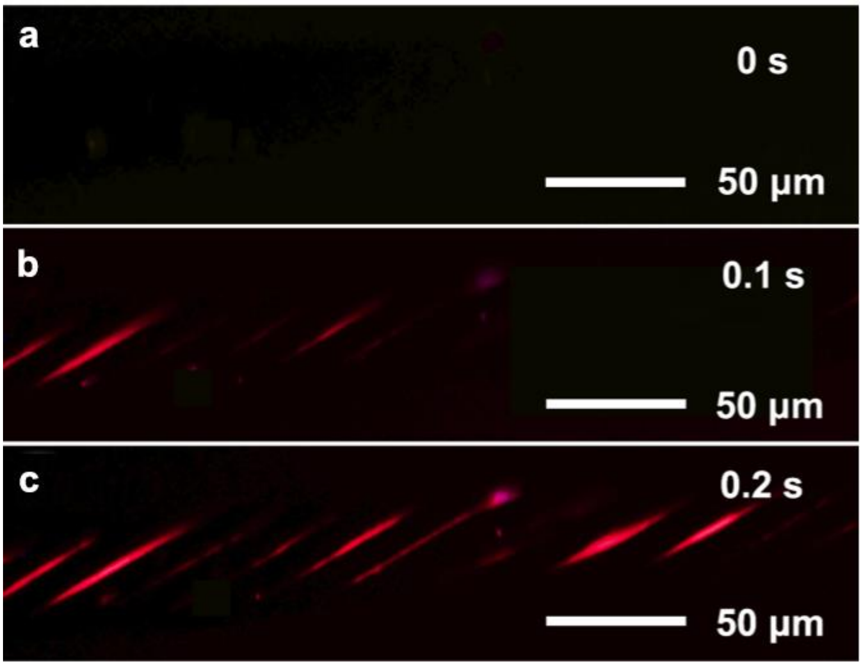

Figure S18 a-c) Fluorescent micrographs in tracing the infiltration of the rhodamine/water solution into the micron-scale channels of an HSF twisted from ten-ply HPFs.

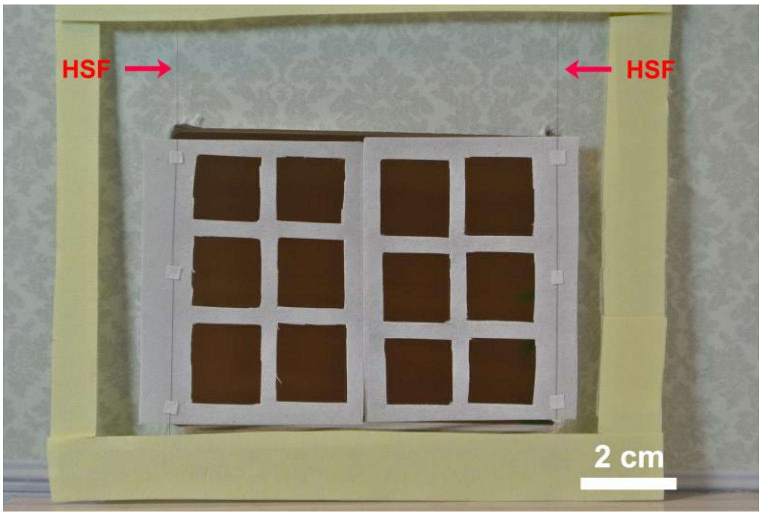

Figure S19. Photograph of the smart window in response to the water. An HSFs was twisted from ten HPF fibers.

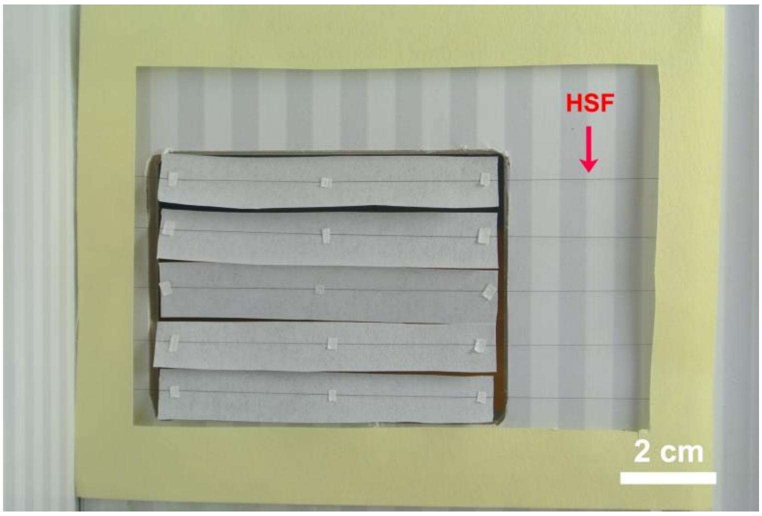

Figure S20. Photograph of the smart louver in response to the change of humidity. An HSF was twisted from ten HPF fibers.

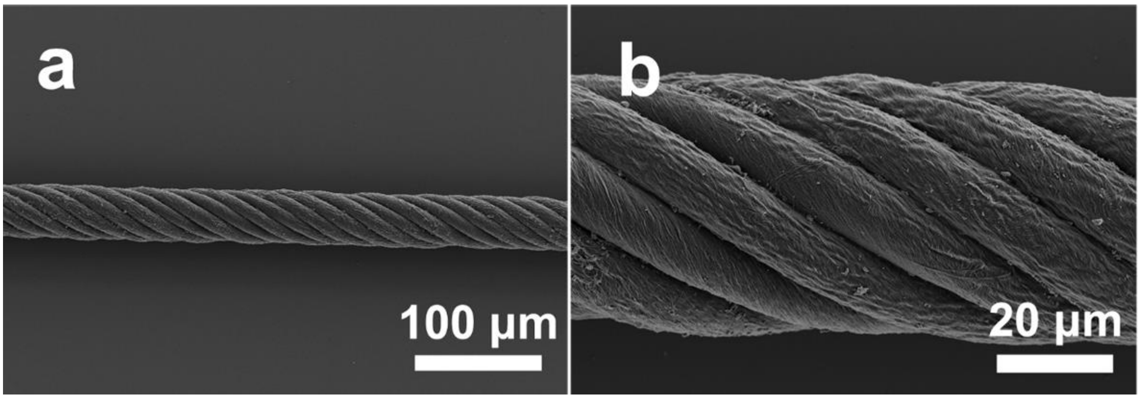

Figure S21. SEM images of a right-handed HSF at low (**a**) and high (**b**) magnifications. The HSF was twisted from ten HPF fibers.

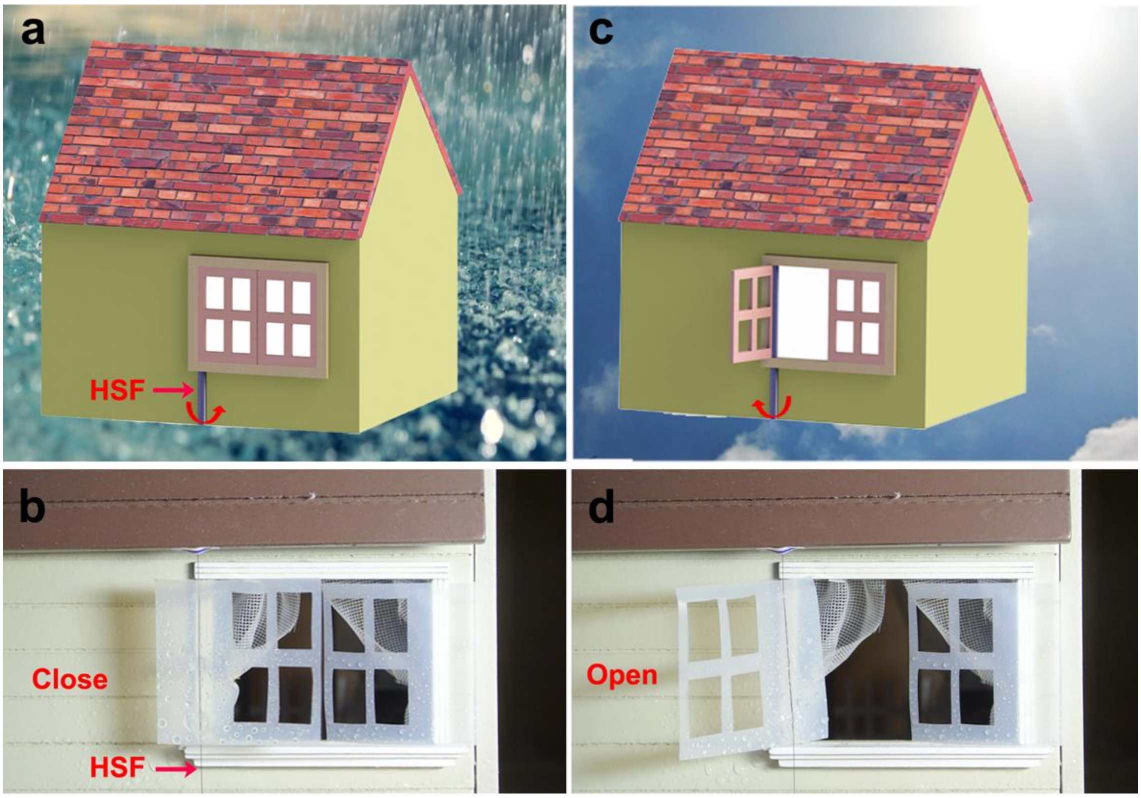

Figure S22. Schemes and photographs of the smart window at closed (**a**, **b**) and opened (**c**, **d**) states. The HSF was twisted from ten HPF fibers.